Hindawi
Journal of Advanced Transportation
Volume 2024, Article ID 9411726, 19 pages
https://doi.org/10.1155/2024/9411726

Research Article

Optimal Mandatory Lane-Changing Location Planning for CAV Based on Cell Transmission Model

Gao Gao,[1,2] **Zhengfeng Huang**,[1,2] **Wei Ji**,[1,2] **and Pengjun Zheng**[1,2]

[1]*Faculty of Maritime and Transportation, Ningbo University, Ningbo 315000, Zhejiang, China*
[2]*Collaborative Innovation Center of Modern Urban Traffic Technologies, Southeast University, Nanjing 211189, China*

Correspondence should be addressed to Zhengfeng Huang; huangzhengfeng@nbu.edu.cn

Received 22 December 2023; Revised 5 March 2024; Accepted 14 March 2024; Published 30 March 2024

Academic Editor: Laura Garach

If dedicate a lane to connected autonomous vehicle (CAV) on a multilane road, the traffic congestion and safety risks remain a major problem but in a different style. Random and disorderly mandatory lane-changing behaviour before approaching the next ramp or intersection would have a disturbing effect on the following vehicles of the traffic flow. This paper mainly establishes the optimal mandatory lane-changing location matching model for each target vehicle in the dedicated CAV lane environment. The aim is to minimizing the total travel time, which could take the disturbing effect into account. This model nests the cell transmission model (CTM) to describe vehicle running. The constraints include the relation between target CAV lane-changing cell and the corresponding behaviour start time, the updating of the flow, and occupancy for varied cells. We use the Ant Colony Optimization (ACO) algorithm to solve the problem. Through the case study of a basic two-lane road scenario in Ningbo, we acquire the convergence results based on the ACO algorithm. Our optimal lane-changing location matching scheme can save 5.9% total travel time when compared to the near-end location lane-changing scheme. We test our model by increasing the total number of upstream input vehicles with 4%, 11%, 15%, and the mandatory lane-changing vehicles with 60%, 200%, respectively. The testing results prove that out optimization method could deal with varied road traffic flow situations. Specifically, when the traffics and mandatory lane-changing vehicles increase, our method could perform better.

1. Introduction

To realize the coordinated optimization of vehicles, roads, and networks to alleviate related traffic problems, governors and researchers are actively exploring road environments suitable for connected autonomous vehicles (CAV). They found that CAV-related road environment could be expected to achieve multiple purposes: (1) Improve road capacity [1]. The road capacity would become higher as the CAV penetration in the mixed traffic flow increases [2]. Collaborative adaptive cruise control (CACC) would contribute to improve road capacity by 21% and 80%, when the market share of CAV is 50% and 90%, respectively [3]. (2) Improve traffic efficiency. CAV can improve traffic efficiency because of the advanced sensing and communication equipment in the vehicle networking system [4]. Lee et al. used VISSIM simulation to obtain a result that the network total network time is saved by 16% and the network average speed is improved by 15.7%, under the condition of 30% CAV penetration [5]. (3) Reduce traffic accident rate. Li et al. proved that the collision risk of freeway can be reduced by 36.5%~98.5%, through the coordinated deployment of CACC and road variable speed limit strategies [6]. (4) Reduce energy consumption. Gawron et al. found that the functions in the CAV-enabled smart transportation system, such as energy-saving driving, fleet driving, and smart intersection, can save about 9% energy consumption [7].

Before CAV market penetration rate reaches 100%, mixed flow of CAV and human-driven vehicle (HV) would be a long-lasting state. How to coordinate these two traffic flows is an important issue. Because of lack of connected communications, HV cannot communicate with surrounding vehicles, traffic lights, and other traffic detection devices. So, the mixed traffic situation is more complicated,

and it is more likely to cause new types of congestion, traffic accidents. Currently, although it is still difficult to set up the CAV operating environment for all lanes in the whole road network, it is relatively feasible to design dedicated CAV lanes for some highways and main roads. The dedicated lane can greatly reduce traffic complexity from separating CAV and HV onto different lanes. Besides, lots of studies propose that the CAV should drive on dedicated lanes, which can alleviate coordination problem related to the car following interactions between CAV and HV. Talebpour et al. found that dedicated CAV lanes perform better in the aspects of travel time reliability and traffic congestion levels, when comparing varied CAV management strategies [8].

However, the introduction of dedicated lanes for CAVs inevitably disrupts the established balance of the existing traffic system, causing diverse sensitivity reactions, especially when some CAVs exit the dedicated lane to enter a regular lane, such as highway exits or main road intersections [9, 10]. When there is a reduction in road capacity within these areas, CAVs tend to make more mandatory lane changes (MLC) within these intricate zones [10]. Without proper regulation, this surge in behaviour can result in unstable traffic flow, backward congestion propagation, congestion diffusion to alternative paths, and even a cascading failure of the road network [11, 12].

In response to the negative impacts on the road traffic system caused by dedicated lanes for CAVs, this study aims to establish the optimal mandatory lane-changing location matching model for each target vehicle in the dedicated CAV lane environment. The goal is to minimize traffic disturbances and prevent potential congestion-related issues.

2. Literature Review

2.1. Lane Changing Control Strategy in CAV Environments. In the realm of CAV, the development of an effective lane changing control strategy is paramount for ensuring safe, efficient, and coordinated movement within the traffic flow. Regarding the controller structure, control strategies can be classified into two categories: trajectory planning-tracking (which includes both a trajectory planning stage and a trajectory tracking stage) and integrated lane change control strategies [13]. The trajectory planning-tracking control strategy is used to achieve the minimum impact on external traffic by determining the optimal time for lane-changing maneuvers and planning the longitudinal trajectory of the vehicle following the lane change [14]. This control strategy is more complex and is typically employed for microlevel control of individual CAV integrated lane change control strategies are typically used for macrolevel control, where they operate by controlling various aspects such as speed, acceleration, time, and trajectory to achieve objectives such as minimal delays, smooth traffic flow, and comfortable driving experience [15, 16]. This control strategy model is relatively simpler and is more suitable for scenarios with simpler road environments and higher vehicle densities.

2.2. Lane Changing Models in CAV Environments. Based on the above vehicle control theory, a series of vehicle control models are proposed. Due to the lack of real-world CAV exposure data, research studies in CAV operation mostly rely on traffic simulation technology. The current simulation models for vehicle lane-changing primarily focus on microscopic simulation. They generally concentrate on the decision details of each vehicle and accurately update its position and car-following gap distance at each discrete interval. Mainstream lane-changing models include the Cellular Automata Model [17, 18], the Gipps model employing multiple factors [19, 20], game theory models between target and influenced vehicles [21, 22], the MOBIL model based on safety-incentive dual criteria [23], and artificial intelligence models represented by fuzzy logic and neural networks [24]. Additionally, some studies have incorporated more realistic factors, such as differences in driving tendencies based on varying speed profiles and the impact of roadway conditions [25, 26].

Although these lane-changing models in a CAV environment can portray vehicle trajectories more realistically, the speed of simulation is very slow because the simulation perspective is very detailed microscopic. CAV needs real-time driving instructions to ensure safe, orderly, and efficient movement of vehicles. However, there is generally a long-time lag in waiting for lane-changing decision feedback through microscopic simulation [27]. This time-consuming process would not meet the response requirement related to dynamic decision-making in the CAV environment. Therefore, some researchers have begun to employ meso-macro traffic simulations [28].

2.3. Application of CTM in CAV Environments. The CTM stands as a robust model, renowned for its simplified formulation and macroscopic approach, enabling the modelling of large-scale networks encompassing various factors [29]. Within CAV-related research, the CTM model typically delineates the trajectories of both CAVs and HVs in mixed traffic flows [30, 31]. These studies predominantly focus on longitudinal flow evolution, utilizing an extended CTM framework to discern the genesis and dissipation of shock waves and queues within CAV-mixed traffic dynamics. However, the utilization of CTM in modelling lateral traffic flow evolution remains relatively constrained, with Pan et al. being one of the few to propose a multiclass multilane cell transmission model [32]. This model incorporates the minimum headway acceptance criteria for lane-changing maneuvers by both vehicle types, thereby enabling the simulation of lane-changing behaviours of CAVs and HVs within mixed traffic environments. This illustrates the potential applicability of CTM across various traffic flow scenarios. We seldom see using CTM to conduct the MLC location matching work.

Building upon this literature foundation, our study seeks to enhance computation efficiency and enable real-time CAV command transfer. Taking a mesomacro level

approach, we use dedicated CAV lane as the scenario and nest the CTM to establish the MLC location matching model for the quasi-off-lane CAV and then solve the model by adopting the Ant Colony Optimization (ACO) algorithm, thereby addressing potential safety and congestion risks associated with dedicated CAV lanes and improving traffic efficiency.

3. Model Establishment and Algorithm Design

3.1. Scenario Creation for Dedicated CAV Lanes. The dedicated CAV lanes can be arranged in road scenarios with no less than two lanes. Varied numbers of lanes make little difference in our optimization method proposal. To facilitate model expression, a two-lane scenario is used for analysis in this paper. A two-lane road scenario is established as shown in Figure 1(a), which consists of the ordinary lane $L1$ and the dedicated CAV lane $L2$. Each lane is divided into cells with the same length. The cell numbers are arranged from small to large according to the direction of traffic flow.

In this paper, we allow the vehicle to leave dedicated CAV lane to ordinary lane but not consider the opposite lane-changing behaviour. If a CAV wants to enter the dedicated lane, it would not be a mandatory behaviour. It could find a chance of large spatial gap between neighbour vehicles to change the lane, thus not affecting the stable operation of CAVs in the dedicated lane. So, the opposite lane-changing behaviour is not the major factor contributing to the potential change in traffic efficiency. It is the reason why we do not consider this factor when modelling.

According to our lane-changing direction assumption, the two-lane road scenario could be changed to the cell diagram of Figure 1(b). Table 1 explains the three types of cells. Lane-changing cell i ($i = 1, \ldots, I$) is a specific design, that only the matched CAV has the right to use the red arrow to enter the neighbour lane.

3.2. Model Construction of an Optimal Mandatory Lane-Changing Location Matching Model

3.2.1. Restatement of the Question. The proposed work is like to assign lane-changing locations to each CAV who is previously on the dedicated lane but must diverge from the roadway in the next link. It means that the vehicles are matched to the individual cells and are forcibly ordered to change lanes at these locations. This method is used to minimize the negative impact on both the traffic operations on dedicated and nondedicated lanes, provided that the CAV and lane-changing cell are effectively matched. We propose to discretize the entire road section before the off-ramp or intersection into I equal cells and assign J CAVs with MLC demand on the dedicated lane to n cells to change lane. The objective function of the model is minimizing the system total travel time for all vehicle groups, where the calculation of vehicle travel time in each cell is the key issue. We intend to acquire the travel time information through the vehicle occupancy and flow updating process in the CTM. Specifically, we construct lane-changing time by correlating it with the CAV speed before the MLC starting, the CAV and HV speeds in the affected area of MLC (indirectly related to the car-following gap distance), etc. Furthermore, all parameters mentioned in this chapter, along with their meanings, have been compiled into a table and included in Table 2 for easy reference.

We make the following assumptions to delineate the conditions under which the model is applicable and to simplify the analysis process:

(1) Each cell could only accept at most one vehicle for lane changing.

(2) The front vehicles are arranged to change lanes in the front cells. It can contribute to preventing lane-changing movement disorders.

(3) The vehicle will not encounter any emergency situations during the lane-changing process, such as a nonyielding vehicle behind the changing vehicle on a regular lane.

(4) No lane change is allowed in the upstream subsection.

3.2.2. Model Description. This optimization model is based on the lane-based CTM model, and we construct a schematic diagram of merging and diverging of two-lane cells as shown in Figure 2 It is longitudinally divided into cells such as $i-1$, i, and $i+1$. $L1$ and $L2$ represent lanes 1 and 2 separately. If cell i on lane 2 is a lane-changing cell, then $x_{i,L1}^{t}$ represents the occupancy in cell i on lane 1 at time interval t, $u_{i,L1}^{t}$ represents the sending flow from cell i to cell $i+1$ on lane 1 at time interval t, and $\bar{u}_{i,L2}^{t}$ represents the lane-changing flow from cell i to cell $i+1$ at time interval t.

3.2.3. Triggering Lane-Changing Behaviour Start Time by the Arrival of Target Connected and CAV. If a CAV is matched to a certain cell to change lane, it is necessary to determine when the CAV enters the corresponding cell to start the lane-changing process. It is because this time directly affects the simulation results of the CTM at adjacent time intervals in the neighbour cells. Firstly, this paper records the position sequence number of this CAV in the entire vehicle fleet. In the CAV environment, each CAV is a motion detector. Thus, it is easy to obtain position sequence number of each CAV. Secondly, we record the cumulative number of vehicles passing through the corresponding cell. At last, they are combined to acquire the lane-changing behaviour start time. The relevant constraints are as follows equation (1).

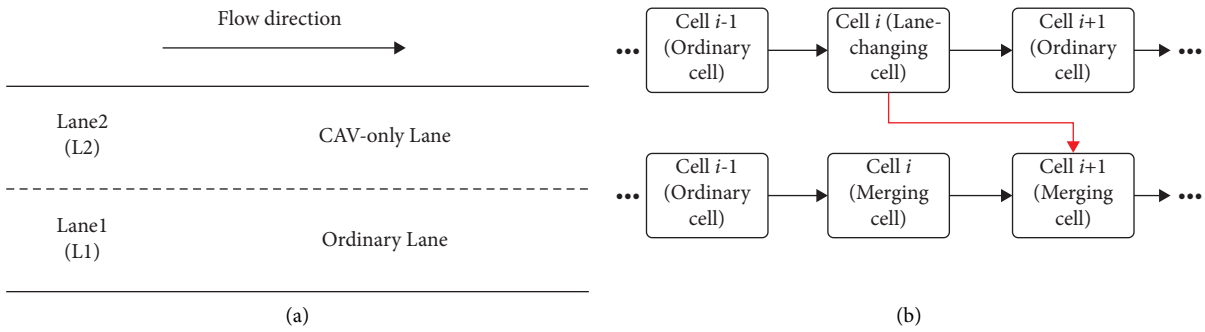

Figure 1: Two-lane road scenario and its cell diagram.

$$\begin{aligned}
&\sum_{j=1}^{J} y_{i,j} \le 1, \quad y_{i,j} \in (0,1)\\
&\sum_{g=1}^{i}\sum_{h=j}^{J} y_{g,h} = 1, \quad \text{if } y_{i,j} = 1\\
&\sum_{t=1}^{n_i-1}\left(u_{i-1,L2}^{t}\right) + \sum_{g=1}^{i-1}\sum_{h=1}^{j-1} y_{g,h} < k_{i,j}, \quad \text{if } y_{i,j} = 1\\
&\sum_{t=1}^{n_i}\left(u_{i-1,L2}^{t}\right) + \sum_{g=1}^{i-1}\sum_{h=1}^{j-1} y_{g,h} \ge k_{i,j}, \quad \text{if } y_{i,j} = 1,
\end{aligned} \tag{1}$$

where $y_{g,h} = 0$ is a variable that judges whether vehicle g changes lane in cell h. If they are matched, then $y_{g,h} = 1$; otherwise, $y_{g,h} = 0$. $y_{g,h}$ acts as a decision variable in our model. The first two lines of equation (1) depict the aforementioned queue rule (the front vehicles are arranged to changes lanes in the front cells), where J is the total CAVs that would change lane in this link. The last two lines tell us how to calculate the lane-changing behaviour start time. In these two inequalities, $k_{i,j}$ denotes the number of all vehicles between vehicle j and the rear of cell i at the beginning of the simulation on dedicated lane. It is also called the relative position sequence number of vehicle j. n_i is the time interval when cell i starts the procedure of lane-changing. The third and fourth inequalities together could contribute to the solving of n_i. The third inequality means that the total receiving flows before time interval n_i plus the total vehicles that have changed lanes in the upstream cells should be less than the relative position sequence number. The fourth inequality together with the third one could tell us that vehicle j just arrives at target cell i at time interval n_i.

3.2.4. Flow and Occupancy Update of Lane-Changing Cells. The outflow from dedicated CAV lane to ordinary lane on the lane-changing cell could be described as equation (2). If the lane-changing maneuver in the cell i has been provided to one of the CAVs, we named the time between the arrival and left of the matched CAV as the duration of the lane-changing procedure. The condition in the first line of equation (2) could tell us that the variable t is just in the procedure time. During this time, the outflow would be determined by taking the minimum of two quantities. The first constraint reflects the requirement that the lane-changing could be achieved only if the car-following gap distance in the neighbor cell is accepted. The second term means that the outflow should not exceed the maximum receiving flow in cell $i+1$ of the ordinary lane.

$$\bar{u}_{i,L2}^{t} = \begin{cases} \min\left(f\left(\dfrac{l}{x_{i,L1}^{t}} - \alpha_i^t\right), \left(X_{i+1,L1} - x_{i+1,L1}^{t}\right)\cdot\delta\right), & \text{if } \sum_{j=1}^{J} y_{i,j} = 1 \text{ and } t \ge n_i \text{ and } \sum_{h=1}^{t-1} \bar{u}_{i,L2}^{h} = 0, \\ 0, & \text{otherwise.} \end{cases} \tag{2}$$

In equation (2), $X_{i,L1}$ denotes the maximum occupancy in cell i of the ordinary lane. δ is the average speed at which congestion waves propagate upstream within high density regions of the road. It could be expressed as the ratio of the reverse wave speed to the free flow speed. $f(\cdot)$ is a 0-1 variable describing whether the lane change can be achieved, taking 1 if the independent variable is greater than 0 and 0 otherwise. α_i^t is the minimum acceptable gap distance for

Table 1: Cell type description.

Cell type	Description
Lane-changing cell	It is located on the dedicated lane; the matched CAV would leave the lane at this cell
Merging cell	It is located on the ordinary lane; both the cell that receives the lane-changing CAV and its upstream neighbor cell belong to this cell
Ordinary cell	All the cells that do not belong to lane-changing cell and merging cell

Table 2: Model parameters and descriptions.

Parameter	
$L1$	Ordinary lane
$L2$	Dedicated CAV lane
I	Total number of lane-changing cells
$x_{i,L1}^t$	The occupancy in cell i on lane 1 at time interval t
$u_{i,L1}^t$	The sending flow from cell i to cell $i+1$ on lane 1 at time interval t
$\bar{u}_{i,L2}^t$	The lane-changing flow from cell i to cell $i+1$ at time interval t
$y_{g,h}$	A variable that judges whether vehicle g changes lane in cell h
J	The total CAVs that would change lane in this link
$k_{i,j}$	The number of all vehicles between vehicle j and the rear of cell i at the beginning of the simulation on dedicated lane
n_i	The time interval when cell i starts the procedure of lane-changing
$X_{i,L1}$	The maximum occupancy in cell i of ordinary lane
δ	The average speed at which congestion waves propagate upstream within high density regions of the road
α_i^t	The minimum acceptable gap distance for lane change
l	Cell length
$Q_{i,L2}$	The flow capacity in cell i of ordinary lane
$\bar{k}_i^t$	The total number of vehicles driving in front of CAV j in cell i at time interval t
$g_{\min}$	The minimum safe following distance
l_i	The average follow-up headway in cell i
γ_i^t	Vehicle equivalent used to quantify the space
σ	Unit time interval length
T	The total number of time intervals

lane change. Its calculation would be depicted in the next subsection. l is the cell length.

Straightforward flow of cell i during the lane-changing procedure could be described as the first line of equation (3). It is determined by not only the general flow, capacity, and remaining occupancy but also the situation that whether the target CAV has arrived at the ordinary lane or not. The last line of equation (3) could depict two conditions. One is at the time before target CAV arrival or after lane change. The other is for ordinary cells on dedicated lanes. Although we put their flow update equation in the framework of lane-changing cell, it would not influence the calculation result.

$$\begin{aligned} u_{i,L2}^t &= \min\left(x_{i,L2}^t - 1, Q_{i,L2}, Q_{i+1,L2}, \left(X_{i+1,L2}^t - x_{i+1,L2}^t\right)\delta, \left(1 - \bar{u}_{i,L2}^t\right) \cdot \bar{k}_i^t + \bar{u}_{i,L2}^t \cdot M\right), \\ &\text{if } \sum_{j=1}^{J} y_{i,j} = 1 \text{ and } t \geq n_i \text{ and } h = 1t - 1\bar{u}_{i,L2}^h = 0 \\ u_{i,L2}^t &= \min\left(x_{i,L2}^t, Q_{i,L2}, Q_{i+1,L2}, \left(X_{i+1,L2} - x_{i+1,L2}^t\right)\delta\right), \text{otherwise}, \end{aligned} \tag{3}$$

where $Q_{i,L2}$ denotes the flow capacity in cell i of the ordinary lane. M is a constant taking a very large quantity. $\bar{k}_i^t$ denotes the total number of vehicles driving in front of CAV j in cell i at time interval t. If the target CAV does not successfully change the lane, the flow received by the downstream cell of the dedicated lane would be constrained by $\bar{k}_i^t$, and $\bar{k}_i^t$ is calculated as the following equation:

$$\bar{k}_i^t = x_{i,L2}^t - \sum_{t=1}^{n_i}\left(u_{i-1,L2}^t\right) - \sum_{g=1}^{i-1}\sum_{h=1}^{j-1} y_{g,h} + k_{i,j}, \text{if } \sum_{j=1}^{J} y_{i,j} = 1 \text{ and } t \geq n_i \text{ and } \sum_{h=1}^{t-1} \bar{u}_{i,L2}^h = 0. \tag{4}$$

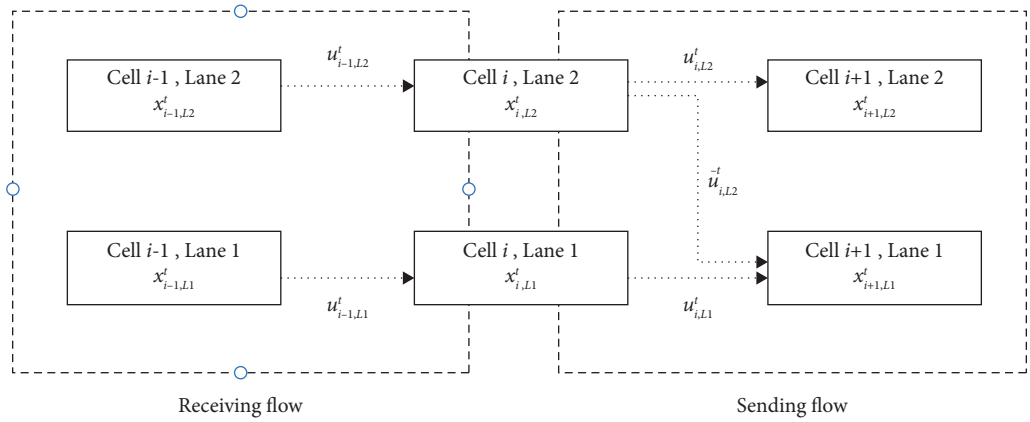

Figure 2: Schematic diagram of merging and diverging cells caused by lane-changing maneuvers.

The occupancy update equation for lane-changing cell i is as the following equation:

$$x^{t+1}_{i,L2} = x^t_{i,L2} + u^t_{i-1,L2} - u^t_{i,L2} - \bar{u}^t_{i,L2}, \tag{5}$$

where $x^t_{i,L2}$ denotes the occupancy of cell i on the dedicated lane at time interval t. The above equation shows that the current cell occupancy is equal to the previous cell occupancy plus the receiving flow minus the outflow due to straightforward propagation and lane-changing behavior.

3.2.5. Flow and Occupancy Update of Merging Cells

(1) Calculation of Minimum Acceptable Gap Distance for Lane Change. The minimum acceptable gap distance α^t_i for MLC is a significant parameter influencing the CTM. For instance, equation (2) used it to check whether the lane-changing flow could be sent. Moreover, although it is permitted to send, the effect of this lane-changing behavior on the downstream flow in the ordinary lane is unknown. We could use α^t_i to express this influence.

Mathematically, the variable α^t_i is related to the minimum safe following distance $g_{\min}$ for vehicles, the speed difference $(v_2(t) - v_1(t))$ between two lanes, and the relative position with reference to the off-ramp or intersection spot (see Figure 3, we use the remaining distance $d(t)$ to depict it). Specifically, apart from gap acceptance criterion and lane speed difference, the matched vehicle with MLC intention is also affected by the remaining distance. The remaining distance $d(t)$ refers to the distance from the current position of the matched vehicle to its target off-ramp or intersection spot. This distance is directly related to the driver's assessment of level of urgency associated with her/his MLC intention. The level of urgency is considered to follow three sequential stages as the vehicle approaches its target turning point [33, 34]. These three stages are separated by two critical positions d_r and d_c. Take a vehicle intending to execute a MLC as example, the target turning point is considered to be remote as long as the remaining distance $d(t) > d_r$, and close if $d(t) < d_c$, where d_r and d_c are distances that define the range within which the variable α^t_i linearly varies from the upper bound to the lower one based on the current speed difference $v_2(t) - v_1(t)$.

$$\alpha^t_i = \begin{cases} c_l \cdot h\left(v_2(t) - v_1(t)\right) + c_f \cdot h\left(v_1(t) - v_2(t)\right) + g_{\min}, & \text{if } d(t) > d_r, \\ \left\{c_l \cdot h\left(v_2(t) - v_1(t)\right) + c_f \cdot h\left(v_1(t) - v_2(t)\right)\right\} \cdot \dfrac{d(t) - d_c}{d_r - d_c} + g_{\min}, & \text{if } d_c \le d(t) \le d_r, \\ g_{\min}, & \text{if } d(t) < d_c, \end{cases} \tag{6}$$

where the function $h(x)$ is defined as equation (7).

$$h(x) = \begin{cases} x, & \text{if } x \ge 0, \\ 0, & \text{if } x < 0. \end{cases} \tag{7}$$

The constant c_l and c_f presents relationship between speed difference with extra leading gap and extra lag gap, when the matched vehicle is still not too aggressive to execute a lane change.

To successfully change lanes, several important factors need to be considered. It would at least include the car following gaps in both lanes, the speed difference between the two lanes, and the extra lag gap, etc. Of course, if it is the MLC in our article, in addition to the above factors, the

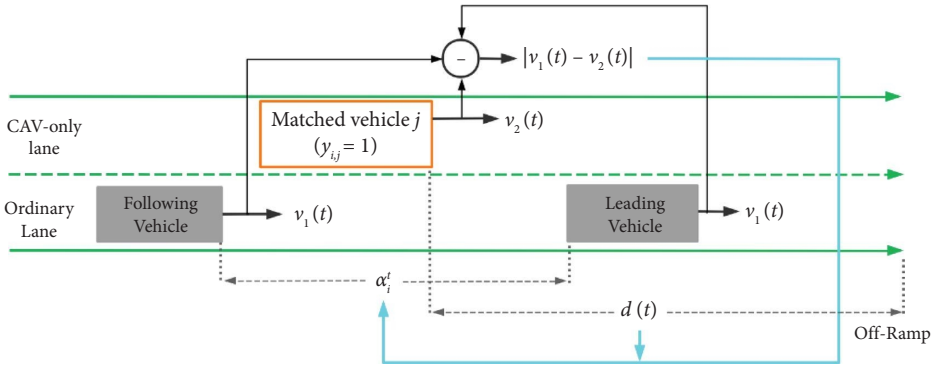

Figure 3: Minimum acceptable gap distance α_i^t and its impact factors.

distance between the current position and the downstream off-ramp should also be considered. This distance is directly related to the driver's assessment of level of urgency associated with her/his MLC intention. Thus, it would affect the minimum acceptable gap for MLC. In our paper, these factors are all considered to a certain extent. However, our simulation model is limited to the characteristics of meso-macro perspective. When considering the car following gap, it is not as much detail as microsimulation can. But even so, it does not affect the fidelity of the lane changing operation. The reasons are as follows.

As to CAV lanes, we do not need to think too much of the car-following distance influence when changing lanes. Because all CAVs are controlled by CAV data center and their speeds can be simultaneously adjusted. When changing lanes, other CAVs can accelerate and decelerate simultaneously to avoid traffic safety problems.

As to ordinary lanes, although we have set a minimum acceptable gap based on speed difference, an issue is that how to keep enough distance between the MLC vehicle and the vehicle behind (also called extra lag gap). Generally, if the speed of the following vehicle is lower than MLC vehicle, then it is not likely to cause collision risk. This time the extra lag gap is not an important factor. However, if the speed relation is opposite, then it is dangerous to change lane without any restriction rule. We add the following rule to deal with this scenario. Relevant legislation can be introduced to ensure the priority right of MLC for CAV. If a high-speed vehicle in the adjacent lanes does not give way to the MLC CAVs, then penalties would be imposed to this vehicle. As to the situation where the CAV speed is lower than the target lane, we use this method to ensure the safety of lane changing. The impact of this measure is mainly reflected in the delay of the following vehicles caused by the deceleration. Fortunately, these impact results have been considered in our objective function.

(2) Allocation of Space for Merging Flow. The vehicles changing lanes will cause disturbance to the upstream vehicles in the target lane. We would allocate more space for merging flow to express this influence. In another words, we use vehicle equivalent (VE) to quantify the space. If l_i is the average follow-up headway in cell i, then the VE γ_i^t could be presented by α_i^t/l_i.

(3) Flow and Occupancy Update of Merging Cells. The occupancy update equation of the CAV merging cell can be obtained as equation (8).

$$x_{i+1,L1}^{t+1} = x_{i+1,L1}^t + u_{i,L1}^t - u_{i+1,L1}^t + \bar{u}_{i,j}^t, \tag{8}$$

where the receiving flow could be expressed as the following equation:

$$u_{i,L1}^t = \max\left[\min\left(x_{i,L1}^t, Q_{i,L1}, Q_{i+1,L1}, \left(X_{i+1,L1}^t - x_{i+1,L1}^t\right)\delta\right), -\gamma_i^t \cdot \bar{u}_{i,j}^t, 0\right]. \tag{9}$$

Multiplying the number of lane-changing vehicles by VE, we could achieve the virtually occupied space $\gamma_i^t \cdot \bar{u}_{i,j}^t$. This space would not be used when calculating the receiving flow from the ordinary lane. In another word, $\gamma_i^t \cdot \bar{u}_{i,j}^t$ quantifies the reduction in the amount of inflow of cell $i+1$ from the ordinary lane due to the perturbation caused by the lane change.

3.2.6. Objective Function Establishment. The objective is to minimize the total travel time of all the participating vehicles in the simulation, which is shown in the following equation:

$$Z = \sum_{t=1}^{T}\sum_{i=1}^{I}\left(x_{i,L1}^t + x_{i,L2}^t\right) \cdot \sigma, \tag{10}$$

where σ is unit time interval length. T is the number of time intervals, which is large enough to allow all vehicles to leave the simulation link.

3.3. Algorithm Steps. The ACO algorithm is a probabilistic algorithm that can be used to find the optimal path in a graph. The heuristic probabilistic search method is prone to find the global optimal solution rather than getting stuck in a local optimum. By establishing the inside heuristic

information function and pheromone intensity update equations, the ACO could be used to solve our model.

When solving this model with the ACO algorithm, the path found by each ant is assumed to be a sequence of cells. Each cell in the sequence is matched to the CAV with lane-changing intention in order of vehicle code. The related algorithm and its annotations are shown in the following steps. Some important steps and the included parameters are described in Algorithm 1.

In this algorithm, two list type variables, CELLTABLE and ROUTETABLE, are used to express the path solutions found by ant colonies. ROUTTETABLE is the transpose of CELLTABLE. Each row of CELLTABLE corresponds to a lane-changing vehicle. Each column represents an ant. Each row of ROUTETABLE corresponds to an ant. Each column represents a lane-changing vehicle. Their elements are matched cells.

The first equation in the algorithm is the equation of transition probability (line 11 in the algorithm). Given a vehicle is matched to a cell, the matching probability of the next vehicle and another cell could be calculated by this equation. In the equation, α is the coefficient of pheromone intensity factor, and β is the coefficient of heuristic information function factor. $\text{allowed}_{r_{k,j-1}}$ contains all the cells whose number is larger than $r_{k,j-1}$. If the cell is out of $\text{allowed}_{r_{k,j-1}}$, then we set the corresponding transition probability to be 0.

We update the heuristic information function as follows (line 20 in the algorithm). Given cell h and i, we should check whether both cells exist in the path found by ant k. If yes, then we should calculate the lane-changing delay in cell i and express it as $\text{delay}_{k,h,i}$. Summing up these delays after searching all ants, we could acquire total delay. It is better to retain the cell i if the total delay is low. In another word, heuristic information value and total delay should be inversely proportional. Thus, we present heuristic information function $\eta_{h,i}$ with the style of line 20.

We update the pheromone intensity by using the previous pheromone and additional pheromone (line 21, 22 and 23 in the algorithm). We use the pheromone volatility factor ρ to reduce the influence of previous pheromone. As to the additional pheromone, it is related to total pheromone Q (a constant) and objective function value Z_k. There is a positive correlation between additional pheromone and Q and a negative correlation between additional pheromone and Z_k. Specifically, even if the ant does not pass the two selected cells together, we should also provide quantity to the additional pheromone. The only difference is that we use a constant W (less than 1, generally adopting 0.5) to control the pheromone value to prevent fast local convergence. In addition, we could constrain the pheromone into a certain range to prevent premature convergence.

4. Case Study

4.1. Case Background. Zhejiang Province in China is currently building "Hangzhou-Shaoyong Wisdom Expressway." The expressway starts from Xiasha interchange in Hangzhou City and ends at Chaiqiao interchange in Ningbo City and has a total length of 175 kilometers. Its long-term goal is to provide a vehicle-road collaborative autonomous driving experience. Besides, since Ningbo Zhoushan port is the world's largest port by throughput volume, the government has the plan to provide a dedicated lane for connected truck platoon to serve efficient road freight transport for this port. In this paper, we select the 13.89 km section from Beilunshan interchange to Chaiqiao interchange (eastbound direction) for analysis. The road is assumed to be a two-lane expressway scenario. We deploy the initial vehicles along the whole road and study the lane-changing subsection from Xiapu interchange to Chaiqiao interchange. Figure 4 shows the map of road section and interchange.

The schematic diagram composed of the two-lane cells based on the study section is shown in Figure 5. The left side of the driving direction is the dedicated CAV lane; the right side deploys the ordinary lane. Assume the free-flow speed and simulation time step to be 100 km/h and 10 s separately, and thus, the length of each cell is approximately 279 m. Since the total length from Beilunshan to Xiapu is 8.33 km, then we could provide 30 cells to divide the lane in this subsection by considering single cell length. We numbered these cells with codes 1, 2, 3, . . ., 30. Similarly, the subsection from Xiapu to Chaiqiao is divided into 20 cells, numbered 31, 32, 33, . . ., 50.

4.2. Parameter Initialization

4.2.1. Vehicle Deployment and Fundamental Diagram in the Cell. The initial vehicle numbers of all cells are generated in a random way, which obey to uniform distribution. Figure 6 shows the initial vehicle numbers on CAV-only lanes and ordinary lanes separately. To analyse the lane-changing influence in the studied subsection (cell 31–50) fairly and objectively, we assume that no lane change is allowed in the upstream subsection and the initial vehicles in the studied subsection would not change lanes.

We should provide the upstream vehicles which have MLC demand in the downstream subsection. These vehicles are shown in the Table 3.

Figure 7 in the example describes the fundamental diagrams of traffic flow on the ordinary lane and the dedicated lane, respectively. These diagrams are also called flow-density trapezoidal relationship graphs. They can reflect the differences with respect of maximum flow, minimum headway, maximum vehicle speed, reverse shock wave propagation velocity, etc. The maximum flow of dedicated lanes and ordinary lanes is 2500 and 1600 veh/h separately, which shows the dedicated lane performs better. The ratio of the unit distance to the traffic density is the headway, and the minimum headway is obtained from the maximum traffic density. Due to the varied maximum traffic densities in the two lanes, the minimum headways are also different. The figures show that the minimum headway in the dedicated lane is smaller than that in the ordinary lane. In addition, the slope between the point in the line and the origin is the vehicle speed. In this three-segment line, when the flow and density are arranged on the first line segment, the maximum vehicle speed can be obtained. It is also named free-flow speed. By comparing the settings of the two fundamental

Input: ant number m, limited iteration number N
Output: CELLTABLE, ROUTETABLE
Initialize list CELLTABLE and ROUTETABLE with lane-changing vehicle $j \leftarrow 2, \ldots, J$ and ant $k \leftarrow 1, \ldots, m$ separately
Initialize the pheromone intensity matrix τ with an all-ones matrix and the heuristic information function matrix η with 0.2
while $n \leq N$ **do**
  $j \leftarrow 1$ //Assign the 1st lane-changing vehicle to j
  $r_{k,j} \leftarrow RAND\ k = 1, \ldots, m$ //For the ant k, match a lane-changing cell to vehicle j, and name the selected cell as $r_{k,j}$
  CELLTABLE $(j) \leftarrow r$//Match m lane-changing cells to vehicle j
  for $(k \leftarrow 1, \ldots, m)$ do
    for $(j \leftarrow 2, \ldots, J)$ do
      $p_{r_{k,j-1},i} \leftarrow (\tau_{r_{k,j-1},i}{}^{\alpha} \cdot \eta_{r_{k,j-1},i}{}^{\beta} / \sum_{h \in \text{allowed}_{r_{k,j-1}}} \tau_{r_{k,j-1},h}{}^{\alpha} \cdot \eta_{r_{k,j-1},h}{}^{\beta}), \quad i \in \text{allowed}_{r_{k,j-1}}$ //Given cell
      $r_{k,j-1}$ is matched to vehicle $j-1$, the conditional probability of selecting cell i to match with vehicle j is shown in this equation
      $r_{k,j} \leftarrow$ Roulette $(p_{r_{k,j-1},i})$ //Acquire the j th matching cell $r_{k,j}$ based on roulette wheel selection
    end
  end
  CELLTABLE $(j) \leftarrow r$
  ROUTETABLE $\leftarrow$ TRANSPOSE (CELLTABLE)
  $Z_k \leftarrow$ Simulate (ROUTETABLE (k)) $k = 1, \ldots, m$ //For the ant k, execute CTM simulation according to equations (1)–(9), and output the objective value Z_k
  $\eta_{h,i} \leftarrow (1/1 + \sum_{k=1\cdots m \text{ and } h,i \in \text{ROUTETABLE}(k)} \text{delay}_{k,h,i}), \forall h < i$ //heuristic information function update
  $\Delta\tau_{h,i} \leftarrow \sum k = 1 \cdots m \text{ and } h, i \in \text{ROUTETABLE}(k) (Q/Z_k)$
  $+ \sum k = 1 \cdots m \text{ and } (h \notin \text{ROUTETABLE}(k) \text{ or } i \notin \text{ROUTETABLE}(k)) (Q \cdot W/Z_k), \forall h < i$
  $\tau_{h,i} \leftarrow (1-\rho) \cdot \tau_{h,i} + \Delta\tau_{h,i}$ //pheromone intensity update
  Update $(Z_{\min})$ //Compare the objective function values of all ants in this iteration and the optimal value in the last iteration, and choose the minimum one as the optimal objective function value of this iteration, and then use its corresponding cell sequence as the optimal solution
  Update n and CELLTABLE and ROUTETABLE as appropriate
end

Algorithm 1: The ACO algorithm.

diagrams, it can be found that the free-flow speed on the dedicated lane is higher than that in the ordinary lane. The slope of the third line segment shows the reverse shock wave propagation velocity δ. They are 40 and 30 km/h separately in these two lanes. The value differences in these indicators can reflect the relative advantages of dedicated lanes.

4.2.2. Parameters of ACO. We set the parameters of the ACO algorithm in Table 4. As to the parameters m, α, β, ρ, and Q, the reference ranges are [1, 10], [1, 4], [0, 5], [0.1, 0.5], and [100, 500], respectively. Table 4 shows the relative feasible input of the parameters after several tests.

4.3. Analysis of Optimization Results

4.3.1. Convergence Process of Iterative Optimization. The process of the system total travel time versus the number of generations is shown in Figure 8. The green line represents the evolutionary curve of the optimal solution, and the blue line represents the mean value of the system total travel time for all solutions under the corresponding iteration. The trend of the total travel time shows that it can eventually converge with the increase of the number of iterations. The optimal total travel time could keep stable after the 750th iteration, indicating that the ACO performs well in solving the model. During the initial 50 iterations, the objective function value decreases rapidly. It is because the randomness and self-organization characteristic of the ACO is more apparent at the beginning of the iterations. In the subsequent iterations, the objective function value decreases more slowly because more pheromones are stacked on the shortest path. These stacked pheromones produce the effect of positive feedback on the historical better solutions, which would be retained in the following iterations. At the last stage of the iteration, since the accumulation of pheromone tends to be stable, the total travel time will not fluctuate greatly. Finally, the optimal system total travel time obtained is 84130 s.

4.3.2. Simulation Results of the Optimal Solution. The matching relationship between the vehicles with MLC demand and lane-changing cells under the condition of optimal solution is shown in Figure 9. The MLC vehicles 1–5 take cells 36, 40, 43, 49, and 50 as the lane-changing locations, respectively. Their lane-changing start times correspond to the 32nd, 35th, 26th, 28th, and 25th time intervals, respectively. Among them, the vehicles in cells numbered 43, 49, and 50 change lanes relatively early because these vehicles are in leading positions initially, and thus, their moving is less affected by other vehicles. In addition, these vehicles are closer to the target cells, which will also contribute to the early start of lane-changing operation.

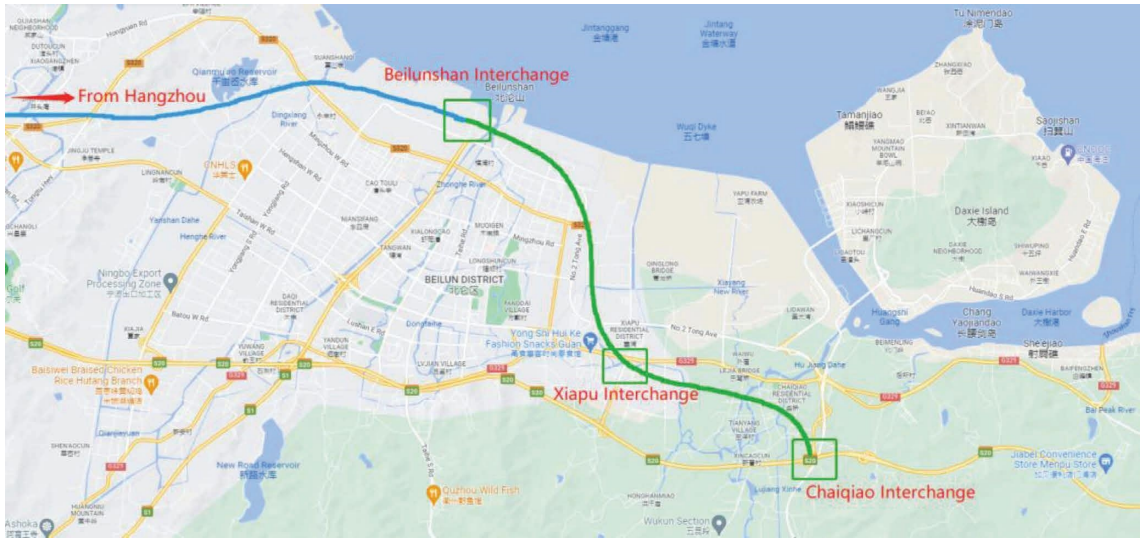

Figure 4: The study section from Beilunshan interchange to Chaiqiao interchange in Hangzhou-Shaoyong wisdom expressway.

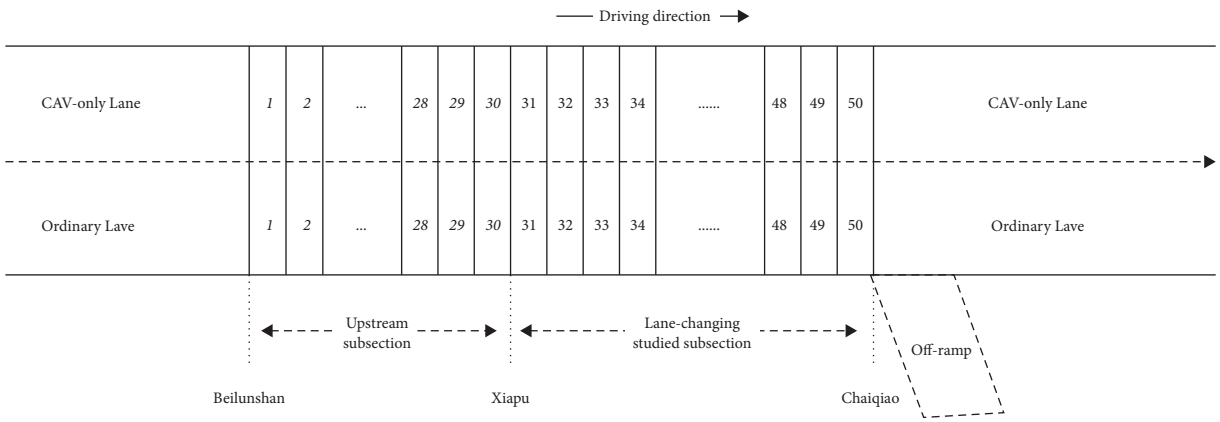

Figure 5: Schematic diagram composed of the two-lane cells.

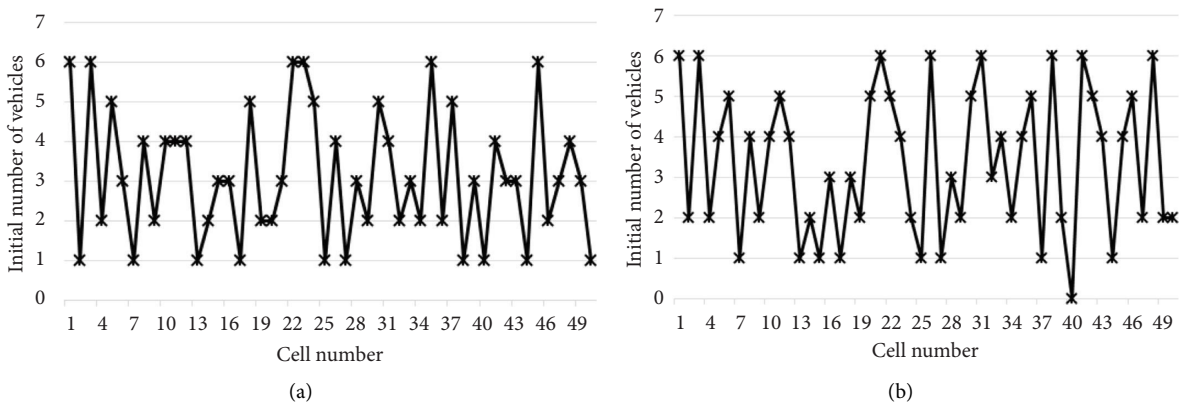

Figure 6: (a) Initial vehicle input in the CAV-only lane; (b) initial vehicle input in the ordinary lane.

To explore the influence of the lane-changing process on following vehicles, we analyzed the accumulative inflow and outflow of the five lane-changing cells. Their flow curves are shown in subfigures of Figure 10, respectively. In order to focus more clearly on the flow variation around the start time of the lane change, horizontal axis values in each graph center on respective lane-changing start time.

In the cumulative inflow-outflow graph, the longitudinal gap between the two curves at a given time interval is the occupancy of the cell. As can be seen from these figures, the

Table 3: The information of the vehicles with MLC demand.

The code for the vehicles with MLC demand	1	2	3	4	5
Its current cell code	2	7	18	22	27
Position sequence number	150	133	100	87	70

Note. The position sequence number of a CAV shows its relative position when arranging the vehicles of a lane from downstream to upstream.

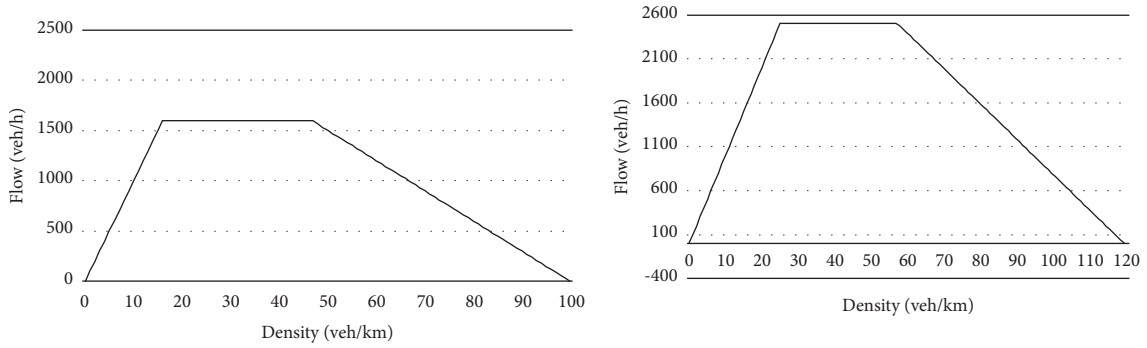

Figure 7: (a) Flow-density relation on the ordinary lane; (b) flow-density relation on the CAV-only lane.

Table 4: Parameter table of ACO.

Parameters	Value
Number of ants (m)	30
Coefficient of pheromone intensity factor (α)	3
Coefficient of heuristic information function factor (β)	1
Pheromone volatility factor (ρ)	0.1
Total pheromone (Q)	100
Maximum number of iterations (N)	1000

longitudinal gaps of these cells at the lane-changing start time are relatively narrow, indicating that the occupancy of the cell is low at this time interval. It also reflects that the MLC vehicles have found good times and locations to execute lane change under the optimal solution. After the lane change is initiated, the inflows of arrival vehicles in the lane-changing cell fail to move forward to the next cell rapidly. Thus, the cumulative outflow curve becomes flat. It results in a wide longitudinal gap between the two curves. As time goes by, the congestion dissipates and the longitudinal curve gaps of most cells get back to normal.

Given the cumulative amount of passed vehicles as a reference, the lateral gap between the two curves is the consumed time for the corresponding vehicle to pass through the current cell. As can be seen from the below parts of these figures, their lateral gaps are relatively narrow. It means that the leading vehicles (in front of the lane-changing vehicles) can pass the cells in less time. However, the vehicles close to the rear of the MLC vehicles take more time to pass the cells due to the influence of lane change. Additionally, vehicles far behind would be less affected by lane changes.

The horn angles formed between the two curves could help evaluate the effectiveness of the solution indirectly. If the angle is small and the horn shrinks early, it means that the traffic flows in these cells move efficiently and the corresponding solution is relatively better. The horn angle and shrinking start time seems well in these figures, which proves the effectiveness of solution.

4.3.3. Comparative Analysis with the Near-End Location Lane-Changing Scheme. The near-end location lane-changing scheme is generally chosen by more drivers for MLC. For instance, Zhang et al. showed that 50% of drivers make a MLC within the 600 m near the freeway off-ramp [35]. However, it would easily cause the phenomenon of lane-changing vehicle bunching. In this paper, we arrange drivers to change lanes in cell 50 to correspond to the near-end location lane-changing scheme. We compare the simulation results of the optimal solution and this scheme as follows.

The total travel time of our scheme and the near-end location lane-changing scheme is 84130 s and 89370 s separately. Our scheme saves the total travel time by 5.9% when compared to the near-end location lane-changing scheme. Besides, the system total delay is 1480 s in our scheme, while it is 6720 s in the compared scheme. Figure 11 shows the cumulative inflow and outflow of cell 50 in the condition of compared scheme. The vehicles (from leading to following vehicle) start to change lanes at time intervals 25, 29, 36, 48, and 55, respectively. It can be found that the lane change behaviour of the MLC vehicle 2 at the 48th time interval causes the largest delay with a total of 890 s. Under our scheme, the maximum system delay caused by a MLC vehicle is only 210 s.

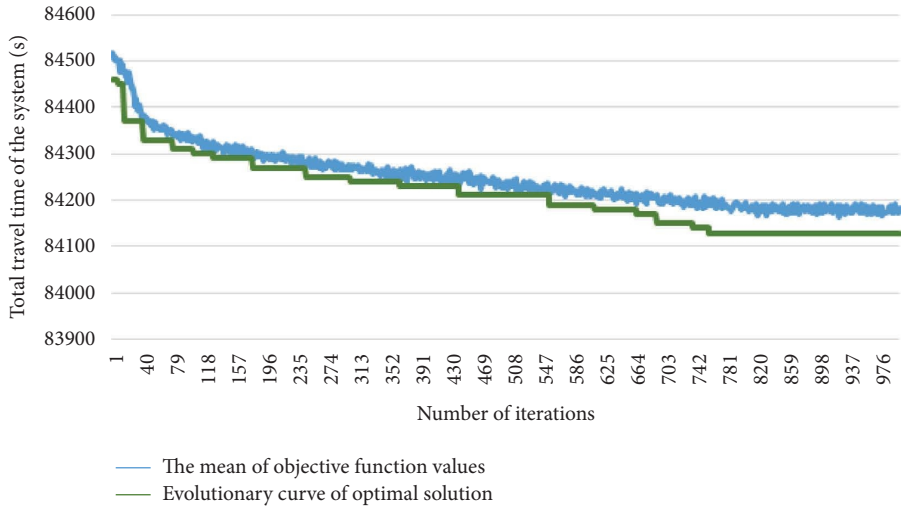

Figure 8: Convergence process of ant colony optimization.

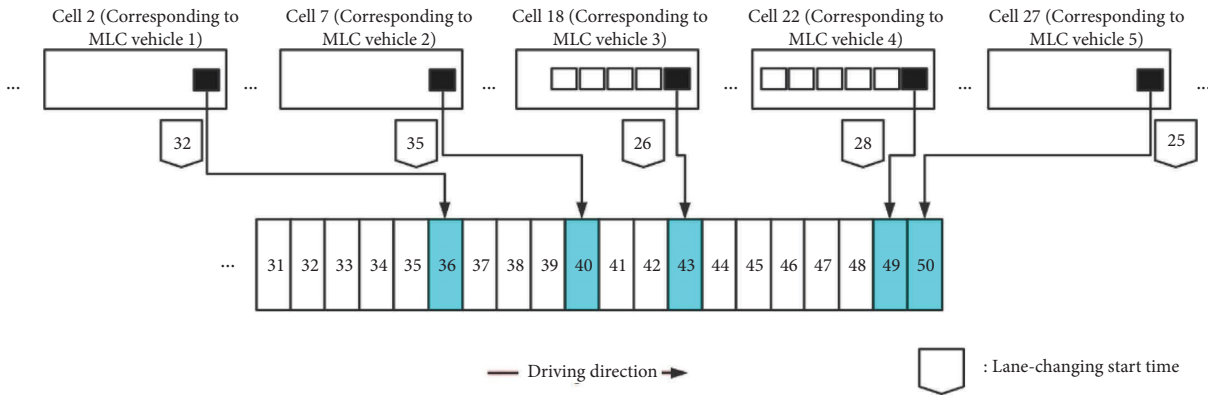

Figure 9: Matching relationship between MLC vehicles and the lane-changing locations.

4.4. Multiscene Application Analysis

4.4.1. System Impact of Varied Upstream Input Vehicles. We would study the change of the downstream lane-changing locations when the number of upstream input vehicles increases. Due to the limitation of cell maximum occupancy, not all upstream cells can increase the number of vehicles. We selected a batch of cells with less initial occupancy for additional vehicle input. According to the initial cell vehicles shown in Figure 6, we select the even-numbered cells within the first 20 cells on the CAV lane, namely, cell 2, cell 4, . . ., cell 18, and cell 20, for vehicle increase. We add 20%, 50%, and 80% more vehicles to these cells, respectively, (the increasing vehicles occupy 4%, 11%, and 15% of the total number of initial vehicles, respectively). We arrange these additional vehicles in the front row of the corresponding cells. The vehicle-cell matched schemes after optimization are shown in Table 5. As the traffics increase, the saving of total travel time in our method also goes upward (from 5.9% to 9.9%) compared to near-end location lane-changing scheme. It means that our method performs better especially when road is congested.

By comparing Figures 9, 12–14, we could clearly find the vehicle-cell matching changes before and after vehicle input variation.

See from the above figures, it can be found that when the number of upstream input vehicles increases by 4%, the 4th and 5th vehicles (in cell 22 and 27 separately) would not change the matched lane-changing cells. When the number increases by 11%, only the 5th vehicle's matching result remains unchanged. When the number increases by 15%, all the matched results are changed. It concludes that the variation of upstream input vehicles has a great impact on the vehicle-cell matching results. But it has less of an impact on the target MLC vehicle if this vehicle is in the front position of the fleet.

It can also be seen that the MLC vehicles' matched cells have a tendency of moving upstream when the number of input vehicles increases. The matched cell number in average is 43.6 when there are no more input vehicles. This average number drops to 41.4, 40.8, and 40.4 when the number of input vehicles increases by 4%, 11%, and 15%. One of the reasons is that when the number of input vehicles increases, the earlier lane-changing behavior will have less of an impact

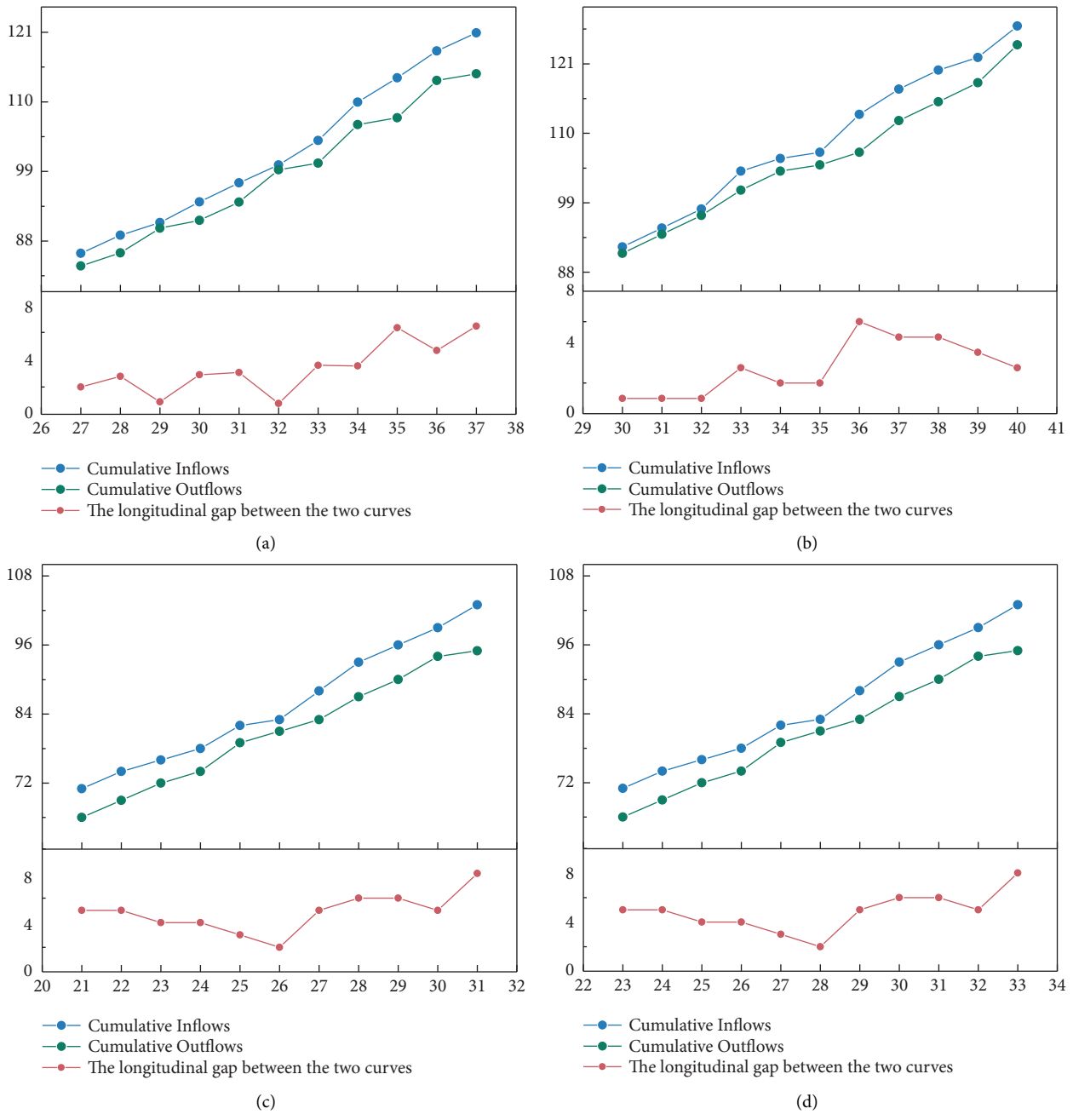

Figure 10: Continued.

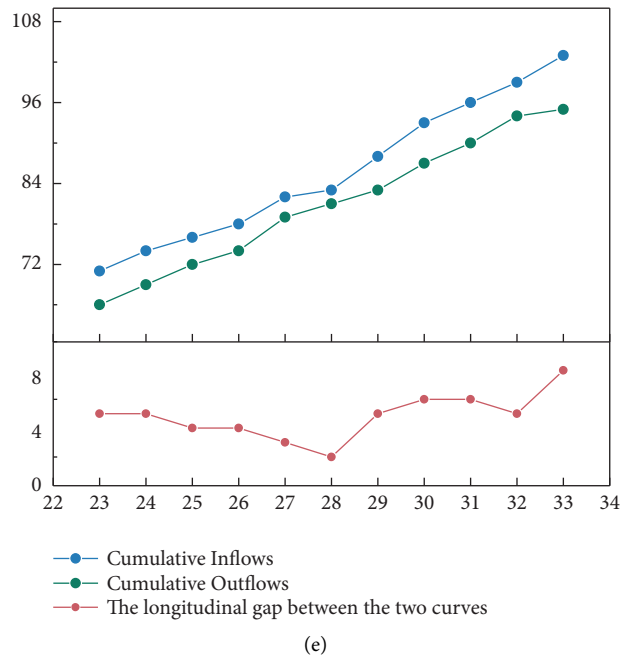

Figure 10: Cumulative inflow and outflow curves of varied cells on the dedicated lane. (a) Cell 36. (b) Cell 40. (c) Cell 43. (d) Cell 49. (e) Cell 50.

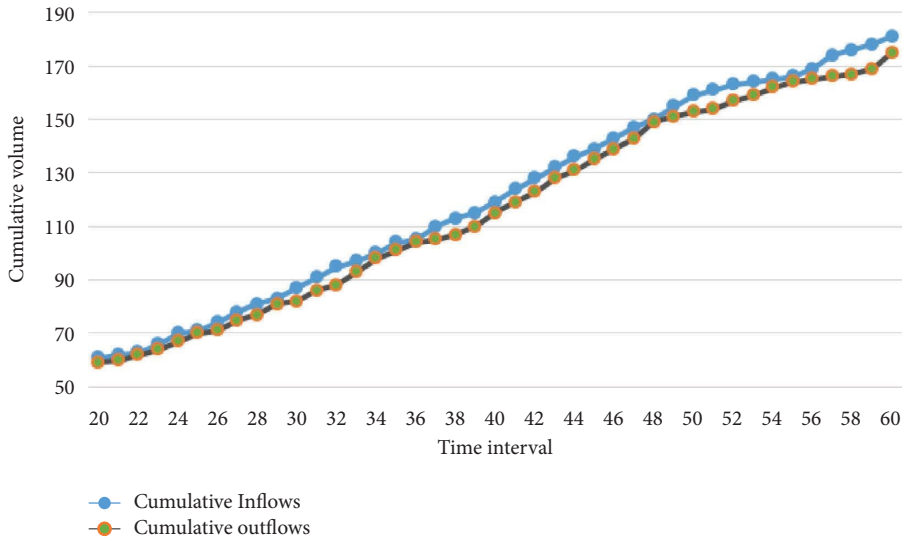

Figure 11: Cumulative inflow and outflow curves of cell 50 on the dedicated lane.

Table 5: Lane-changing location matching schemes under varied upstream input vehicles increases.

Vehicle increasing proportion of the total initial vehicles (%)	The cell number corresponding to the best lane-changing locations	The optimal total travel time of the system (s)	Time saving compared to near-end location lane-changing scheme (%)
0	36, 40, 43, 49, 50	84130	5.9
4	31, 38, 39, 49, 50	85920	6.8
11	31, 34, 43, 46, 50	89060	9.2
15	31, 35, 43, 46, 47	90780	9.9

on the overall system traffic flow operation. So, we could learn that the MLC vehicle would change the lane earlier when the road is congested.

4.4.2. System Impact of Varied MLC Vehicles. We provide two more scenarios of MLC vehicles to explore whether our method could be applied. We increase the number of MLC

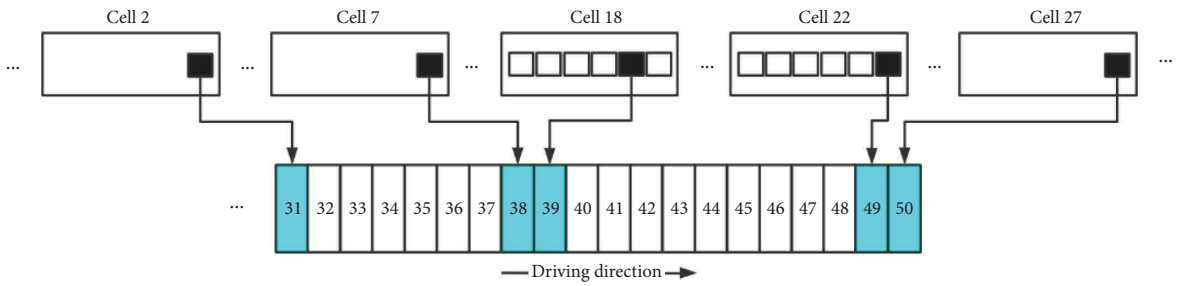

Figure 12: Schematic diagram of the lane changing position for the total number of upstream input vehicles to increase by 4%.

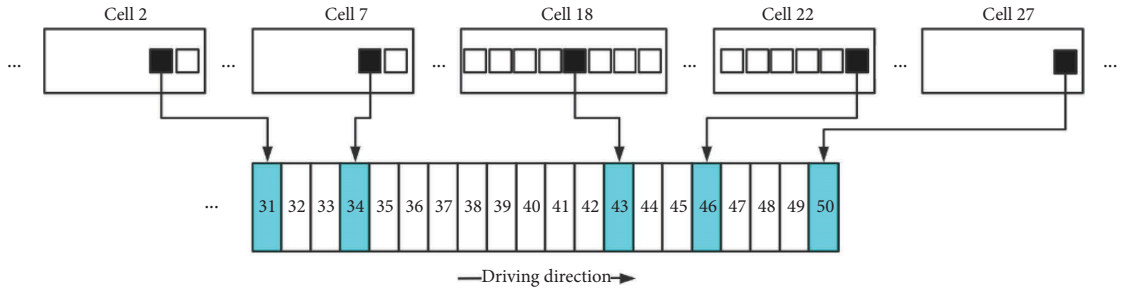

Figure 13: Vehicle-cell matching when upstream input vehicles increase by 11%.

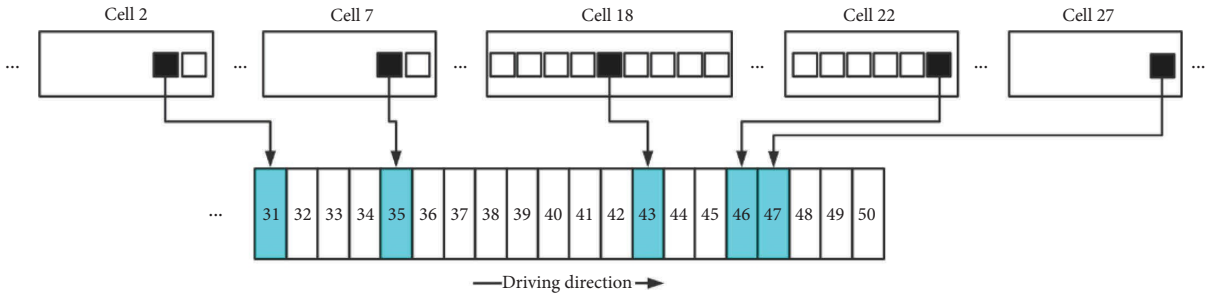

Figure 14: Vehicle-cell matching when upstream input vehicles increase by 15%.

vehicles by 60% and 200%, respectively. It means that the numbers are changed to 8 and 15. The initial position sequences of the expansion MLC vehicles are shown in Table 6.

Table 7 shows the comparison of our method and the near-end location lane-changing scheme in the case of MLC vehicles' expansion scenarios. The system total travel times by our method are 84670 s and 88210 s separately in 8 and 15 MLC vehicles scenarios, which could save time by 6.4% and 11.5% compared to the near-end location lane-changing scheme under the two scenarios. It means that our method performs better especially when MLC demand increases.

5. Discussion

In this paper, the setting of dedicated lanes for CAV and variable sections for MLC could be used for practical engineering application. Our design aims to deploy lateral signal control along the dedicated lanes, while the corresponding sections permit to enable MLC behaviour for the matched vehicles. More specifically, the contribution lies in providing the best locations match for the CAVs with MLC demand, and it is different from the conventional CAV MLC research studies. Some of the previous research studies design lane-changing trajectories for the road of 100% CAV penetration [36, 37], etc. Others focus on the detailed design of lane-changing rules but mostly ignore the impact of these rules on the overall traffic performance [20, 38]. Our research can be applied to mixed-vehicle scenarios, and the optimal MLC location for each CAV is determined by considering the impact of lane-changing behaviour on overall traffic performance. Besides, although the design of the lane-changing rule is not the major focus of this paper, sufficient details have been considered at the level of the mesoscopic traffic simulation model. The model has fully considered the impact of minimum acceptable gap distance requirement and lane-changing behaviour on the following traffic flow in the target lane, making the lane-changing rule relatively feasible. For example, we amplify the virtual outflow of lane-changing vehicles by using the variable of VE γ_i^t, to achieve the hindering effect of the lane-changing behaviour on the following traffic flow. Therefore, this

Table 6: The initial position sequences of the expansion MLC vehicles.

Number of vehicles to change lanes	The initial position sequence of the expansion MLC vehicles (from upstream to downstream)	Cells for MLC vehicles input
8 (+60%)	150, 143, 133, 120, 111, 100, 87, 70	2, 4, 7, 11, 15, 18, 22, 27
15 (+200%)	155, 150, 143, 138, 133, 127, 120, 111, 105, 100, 94, 87, 81, 76, 70	1, 2, 4, 5, 7, 9, 11, 15, 17, 18, 21, 22, 23, 24, 27

Table 7: Comparison of our method and the near-end location lane-changing scheme in the case of MLC vehicles expansion scenarios.

Number of vehicles to change lanes	Cell numbers matched by MLC vehicles	Total travel time (s)	Time saving compared to near-end location lane-changing scheme (%)
8	31, 36, 37, 39, 46, 48, 49, 50	84670	6.4
15	31, 32, 34, 35, 36, 39, 40, 41, 42, 44, 45, 47, 48, 49, 50	88210	11.5

paper has properly considered the criteria of computing efficiency and accuracy in the selection of the simulation model and lane-changing rule. It is a compromise method. In future research, on the basis of not excessively reducing the computing efficiency, we would further incorporate more microscopic lane-changing rules or use real-world data to calibrate the current lane-changing parameters to improve the accuracy of model application.

We use the ACO algorithm to solve the vehicle-cell matching model. Many studies related to the matching of vehicles and road facilities use ACO, and they also validate the feasibility of ACO [39, 40]. ACO can be used for some real-time decision-making problems, due to its fast convergence characteristics in the process of searching for the optimal solution. If people want to quickly obtain the solution of the engineering scheme, perhaps some simple heuristic algorithms such as Latin hypercube sampling could be more recommended. But we cannot guarantee the result validity of these algorithms. Fortunately, we do not need to worry about the validity issue of ACO too much. Our model combined with ACO can reduce the total travel time by 5.9% when compared to the near-end location lane-changing scheme. In future, we would compare ACO with more evolutionary algorithms (such as genetic algorithm) to test its accuracy.

The MLC behaviours would be most likely to occur on the same location near the off-ramp or intersection if no control measure is carried out. It has a negative impact on the safe and stable operation of the traffic system if it is in a congested scenario. Our method could be specifically applied for congested roads. We verify this point by conducting sensitivity analysis. The traffic demand sensitivity results show that if the traffics increase (from 0 to 15%), the saving of total travel time in our method also goes upward (from 5.9% to 9.9%) compared to the near-end location lane-changing scheme. The MLC demand sensitivity results show that if the numbers of MLC vehicles increase to 8 and 15 from 5, the total travel time savings achieve to 6.4% and 11.5% compared to the near-end location lane-changing scheme. So, the performance of our method in congested situation is better than the scene without control measure.

Our vehicle-location matching for MLC is a scheme sent to CAV before it comes to the next link. The CAV has enough time to execute the scheme after entering the next link. So, our research could help traffic engineers implement the real-time traffic control on specific roads. As to the operation, firstly, the CAV data centre should collect CAV dynamic position information. Secondly, this centre should adopt our method to achieve the matching scheme once receiving all the MLC requests about leaving the mainline in the next link. Thirdly, this centre should send the matching information to the screen of the corresponding CAV to achieve in-vehicle information guidance. In conclusion, our research can provide dynamic decision-making assistance for the CAV data centre in improving the efficiency of traffic operation.

About the case of Hangzhou-Shaoyong Wisdom Expressway, in the official scheme design of this road, it indeed mentioned the requirement of reserving a dedicated lane for connected vehicles. It is in line with our application background. However, the road used in this paper is still under construction, so there are some assumptions about traffic flow and so on. The reason why we do not borrow the data from other real scenarios is that some technologies are not yet mature and nearly no such data could be referred to. For example, because the safety problem of autonomous driving has not been completely solved, the penetration rate of autonomous driving vehicles is very low, and the CAV network system is not established, etc. This research is oriented to future scenarios. Since there is no application of data related to the traffic flow of CAV in the real environment, simulation experiment is generally used. Related research studies adopted a hypothetical scenario for analysis [36]. Even if there are real test data, they only design the field with few autonomous vehicles.

If CAVs cannot find the corresponding lane changing space on the HV lanes under some conditions, is the method still useful? When the CAV arrives at the designated place and finds there is not enough gap on the HV lane, the model has set the CAV to slow down or even wait until there is a safe gap to change lane. The delays of itself and the related vehicles have all been taken into account in the model. This situation generally corresponds to the scenario of high vehicle occupancy and MLC CAVs. Any schemes in this situation would produce delays. Our scheme performs better in the aspect of delay when compared to other schemes.

However, these conclusions are based on an assumption. The real-world evolution of future short-term traffic flow is assumed to be close to that from our model. It is possible that the trend of traffic flow is not consistent with our model. Faced with this uncertain traffic development trend, the only thing we can do is to improve the accuracy of our prediction method. For instance, we could shorten the simulation unit time and the cell length. If the traffic flow evolution is unusual, a microsimulation model can be nested to consider more factors to achieve relatively correct flow estimation. Of course, for some extreme traffic development trends, any traffic flow estimation method could not deal with this kind of situation. At this time, some emergency measures need to be taken. For example, if the effect of lane-changing measures is not as good as expected, it is necessary for the data centre to intercept the upstream traffic flow or to instruct the remaining MLC CAVs to change lanes in advance to ease congestion. In conclusion, our model contributes to provide a reference for the lane-changing scheme for the MLC CAVs in nonemergency scenarios.

6. Conclusion

This paper focuses on how to deal with conflict problems arising from the MLC behaviour of CAV in the case of setting up dedicated lanes. If more CAVs conduct MLC behaviour near off-ramps or intersections, it would increase the potential congestion risk and safety hazards. By establishing a MLC location matching model and finding a suitable algorithm to solve it, an optimal MLC location is matched in advance for each CAV on the whole road section. This method could be helpful to the solving of the aforementioned traffic conflict.

To be specific, the MLC location matching model nesting the CTM is constructed to reduce the impact of lane change on following traffic flow and the ACO is used to acquire the result. The model is based on the objective of minimizing the total travel time of all vehicles and the constraints including the vehicle MLC start time, the flow, and occupancy update in varied cells. These constraints are different from the traditional CTM model, especially in the coding of each vehicle and the lane-changing delay calculation.

The feasibility of the model and the algorithm is demonstrated by a two-lane scenario. It shows that objective function convergence can be obtained. Comparative experiments show that the total travel time and vehicle delay under the optimal solution are significantly better than the general near-end location lane-changing scheme. To prove the reliability of our method, the results of the optimal solution are analysed for the scenarios of 4%, 11%, and 15% increase in the total number of upstream input vehicles and 60%, 200% increase in the total demand of MLC. These tests verify the effectiveness of our method. Particularly, the method has much more superiority in congested road.

In future, we should do an in-depth study of how lane-changing from ordinary lane to dedicated lane influence the total travel time. Theoretically, after the dedicated lane receiving the entry request signal from the adjacent lane, the CAV operation centre can adjust the speeds of neighbour vehicles on the dedicated lane to leave enough clearance for the lane-changing vehicle to enter smoothly. It will generally cause few traffic conflicts. As to the potential impacts of these behaviours (this lane change is human's behaviour and thus more complex) on transportation system cost and how to deal with the related optimization of control measure, our future research would pay more attention on these problems. In addition, as to our current research, when the CAV leaves the dedicated lane, the control right would be transferred to the driver. There should be many uncertain disturbance factors influencing the human-computer interaction. We would explore these factors and calibrate related parameters to make the model better resemble real-life scenarios.

Data Availability

Data used to support the findings of this study are available on request.

Conflicts of Interest

The authors declare that they have no conflicts of interest.

Acknowledgments

This study was supported by the "Pioneer" and "Leading Goose" R&D Program of Zhejiang Province: Research on Active Traffic Control Methods and Systems for Highway Networks (2024C01180), the National Natural Science Foundation of China (52272334), the National "111" Centre on the Safety and Intelligent Operation of Sea Bridges (D21013), and the International Scientific & Technological Cooperation Projects of Ningbo (2023H020).

References

[1] K. Brookhuis, D. Waard, and W. Janssen, "Behavioural impacts of advanced driver assistance systems-an overview," *European Journal of Transport and Infrastructure Research*, vol. 1, 2001.

[2] V. A. C. van den Berg and E. T. Verhoef, "Autonomous cars and dynamic bottleneck congestion: the effects on capacity, value of time and preference heterogeneity," *Transportation Research Part B: Methodological*, vol. 94, pp. 43–60, 2016.

[3] S. Shladover, D. Su, and X.-Y. Lu, "Impacts of cooperative adaptive cruise control on freeway traffic flow impacts of cooperative adaptive cruise control on freeway traffic flow," *Presented at the Transportation Research Record: Journal of the Transportation Research Board*, 2012.

[4] M. Kamrani, B. Wali, and A. J. Khattak, "Can data generated by connected vehicles enhance safety? A proactive approach to intersection safety management," *Transportation Research Record*, vol. 2659, no. 1, pp. 80–90, 2017.

[5] J. Lee, J. Bared, and B. Park, "Mobility impacts of cooperative adaptive cruise control (CACC) under mixed traffic conditions," *World congress on intelligent transport systems and ITS America annual meeting*, 2014.

[6] Y. Li, C. Xu, L. Xing, and W. Wang, "Integrated cooperative adaptive cruise and variable speed limit controls for reducing rear-end collision risks near freeway bottlenecks based on

micro-simulations," *IEEE Transactions on Intelligent Transportation Systems*, vol. 18, no. 11, pp. 3157–3167, 2017.

[7] J. H. Gawron, G. A. Keoleian, R. D. De Kleine, T. J. Wallington, and H. C. Kim, "Life cycle assessment of connected and automated vehicles: sensing and computing subsystem and vehicle level effects," *Environmental Science and Technology*, vol. 52, no. 5, pp. 3249–3256, 2018.

[8] A. Talebpour, H. S. Mahmassani, and S. H. Hamdar, "Modeling lane-changing behavior in a connected environment: a game theory approach," *Transportation Research Procedia*, vol. 7, pp. 420–440, 2015.

[9] A. Mittal, R. Twumasi-Boakye, X. Cai, J. Fishelson, Y. Chen, and E. Wingfield, *Assessing the Impacts of Dedicated CAV Lanes in a Connected Environment: An Application of Intelligent Transport Systems in Corktown, Michigan*, SAE International, Warrendale, PA, USA, 2021.

[10] C. Yang, X. Chen, X. Lin, and M. Li, "Coordinated trajectory planning for lane-changing in the weaving areas of dedicated lanes for connected and automated vehicles," *Transportation Research Part C: Emerging Technologies*, vol. 144, 2022.

[11] H. Sha, M. K. Singh, R. Haouari et al., "Network-wide safety impacts of dedicated lanes for connected and autonomous vehicles," *Accident Analysis and Prevention*, vol. 195, 2024.

[12] Z. Wang, D. Sun, M. Zhao, L. Wang, and S. Cheng, "Connected autonomous vehicle control strategy for mandatory lane-changing at intersection: a cyber-physical system perspective," *IEEE Transactions on Intelligent Vehicles*, pp. 1–12, 2023.

[13] K. Sun, X. Zhao, S. Gong, and X. Wu, "A cooperative lane change control strategy for connected and automated vehicles by considering preceding vehicle switching," *Applied Sciences*, vol. 13, no. 4, 2023.

[14] H. Taghavifar and K. Shojaei, "Adaptive robust control algorithm for enhanced path-tracking performance of automated driving in critical scenarios," *Soft Computing*, vol. 27, no. 13, pp. 8841–8854, 2023.

[15] S. Wang, Z. Wang, R. Jiang, F. Zhu, R. Yan, and Y. Shang, "A multi-agent reinforcement learning-based longitudinal and lateral control of CAVs to improve traffic efficiency in a mandatory lane change scenario," *Transportation Research Part C: Emerging Technologies*, vol. 158, 2024.

[16] H. Zhang, L. Du, and J. Shen, "Hybrid MPC system for platoon based cooperative lane change control using machine learning aided distributed optimization," *Transportation Research Part B: Methodological*, vol. 159, pp. 104–142, 2022.

[17] X. Yang, Q. Guo, and Q. Fu, "Decision strategy models of merge influence area for outside vehicles based on vehicle-vehicle communication," *Journal of System Simulation*, vol. 27, pp. 1112–1126, 2015.

[18] C. Dong, H. Wang, Y. Li, W. Wang, and Z. Zhang, "Route control strategies for autonomous vehicles exiting to off-ramps," *IEEE Transactions on Intelligent Transportation Systems*, vol. 21, no. 7, pp. 3104–3116, 2020.

[19] Y. Liu, H. Wang, C. Dong, and Y. Chen, "A centralized relaxation strategy for cooperative lane change in a connected environment," *Physica A: Statistical Mechanics and Its Applications*, vol. 624, 2023.

[20] M. Rahman, M. Chowdhury, Y. Xie, and Y. He, "Review of microscopic lane-changing models and future research opportunities," *IEEE Transactions on Intelligent Transportation Systems*, vol. 14, no. 4, pp. 1942–1956, 2013.

[21] Y. Ali, Z. Zheng, M. M. Haque, and M. Wang, "A game theory-based approach for modelling mandatory lane-changing behaviour in a connected environment," *Transportation Research Part C: Emerging Technologies*, vol. 106, pp. 220–242, 2019.

[22] B. Gong, F. Wang, C. Lin, and D. Wu, "Modeling HDV and CAV mixed traffic flow on a foggy two-lane highway with cellular automata and game theory model," *Sustainability*, vol. 14, no. 10, 2022.

[23] A. Kesting, M. Treiber, and D. Helbing, "General lane-changing model MOBIL for car-following models," *Transportation Research Record: Journal of the Transportation Research Board*, no. 1999, 2007.

[24] Z. el abidine Kherroubi, S. Aknine, and R. Bacha, "Novel decision-making strategy for connected and autonomous vehicles in highway on-ramp merging," *IEEE Transactions on Intelligent Transportation Systems*, vol. 23, no. 8, pp. 12490–12502, 2022.

[25] Z. Huang, D. Chu, C. Wu, and Y. He, "Path planning and cooperative control for automated vehicle platoon using hybrid automata," *IEEE Transactions on Intelligent Transportation Systems*, vol. 20, no. 3, pp. 959–974, 2019.

[26] F. Perronnet, J. Buisson, A. Lombard, A. Abbas-Turki, M. Ahmane, and A. El Moudni, "Deadlock prevention of self-driving vehicles in a network of intersections," *IEEE Transactions on Intelligent Transportation Systems*, vol. 20, no. 11, pp. 4219–4233, 2019.

[27] F. Alasiri, Y. Zhang, and P. A. Ioannou, "Per-lane variable speed limit and lane change control for congestion management at bottlenecks," *IEEE Transactions on Intelligent Transportation Systems*, vol. 24, no. 12, pp. 13713–13728, 2023.

[28] M. Carey, C. Balijepalli, and D. Watling, "Extending the cell transmission model to multiple lanes and lane-changing," *Networks and Spatial Economics*, vol. 15, no. 3, pp. 507–535, 2015.

[29] L. Adacher and M. Tiriolo, "A macroscopic model with the advantages of microscopic model: a review of Cell Transmission Models extensions for urban traffic networks," *Simulation Modelling Practice and Theory*, vol. 86, pp. 102–119, 2018.

[30] Y. Jin, Z. Yao, J. Han, L. Hu, and Y. Jiang, "Variable cell transmission model for mixed traffic flow with connected automated vehicles and human-driven vehicles," *Journal of Advanced Transportation*, vol. 2022, Article ID 6342857, 15 pages, 2022.

[31] W. Tian, "The double lanes cell transmission model of mixed traffic flow in urban intelligent network," *Energies*, vol. 16, no. 7, 2023.

[32] T. Pan, W. H. K. Lam, A. Sumalee, and R. Zhong, "Multiclass multilane model for freeway traffic mixed with connected automated vehicles and regular human-piloted vehicles," *Transportmetrica: Transportation Science*, vol. 17, no. 1, pp. 5–33, 2021.

[33] Q. Yang and H. N. Koutsopoulos, "A Microscopic Traffic Simulator for evaluation of dynamic traffic management systems," *Transportation Research Part C: Emerging Technologies*, vol. 4, no. 3, pp. 113–129, 1996.

[34] T. L. Pan, H. K. W. Lam, A. Sumalee, and R. X. Zhong, "Modeling the impacts of mandatory and discretionary lane-changing maneuvers," *Transportation Research Part C: Emerging Technologies*, vol. 68, pp. 403–424, 2016.

[35] L. Zhang, C. Chen, J. Zhang, S. Fang, J. You, and J. Guo, "Modeling lane-changing behavior in freeway off-ramp areas from the Shanghai naturalistic driving study," *Journal of Advanced Transportation*, vol. 2018,10 pages, 2018.

[36] X. Hu and J. Sun, "Trajectory optimization of connected and autonomous vehicles at a multilane freeway merging area,"

Transportation Research Part C: Emerging Technologies, vol. 101, pp. 111–125, 2019.

[37] Y. Hou, P. Edara, and C. Sun, "Situation assessment and decision making for lane change assistance using ensemble learning methods," *Expert Systems with Applications*, vol. 42, no. 8, pp. 3875–3882, 2015.

[38] K. Nagel, "Two-lane traffic rules for cellular automata: a systematic approach," *Physical Review E-Statistical Physics, Plasmas, Fluids, and Related Interdisciplinary Topics*, vol. 58, no. 2, pp. 1425–1437, 1998.

[39] J. Tang, Y. Kong, Z.-D. Pan, and Y. Dong, "An ant colony optimization algorithm for vehicle routing problem with cargo coefficient," *Mathematical Sciences*, vol. 25, pp. 699–702, 2008.

[40] M. Roca-Riu, E. Fernández, and M. Estrada, "Parking slot assignment for urban distribution: models and formulations," *Omega*, vol. 57, no. PB, pp. 157–175, 2015.